The role of Lagrangian Coherent Structures in development and non-development of tropical cyclones

Blake Rutherford and Michael T. Montgomery
Naval Postgraduate School

June, 2011

Outline

Steady flow approximation in westward propogating pouch

- Pouch travels at approximately the computed translation speed
- After subtracting the translation speed, the flow is approximately steady
- Recirculating streamlines can be seen in the translated reference frame
- These recirculating streamlines may not constrain particle movement in the time-dependent flow

Simplified flow topology

- The manifolds of a hyperbolic saddle form a protective barrier around the pouch
- The unstable manifold wraps around the pouch center in a convergent pouch
- The manifolds form a boundary between the pouch and environmental air masses

Hyperbolic vortex schematic

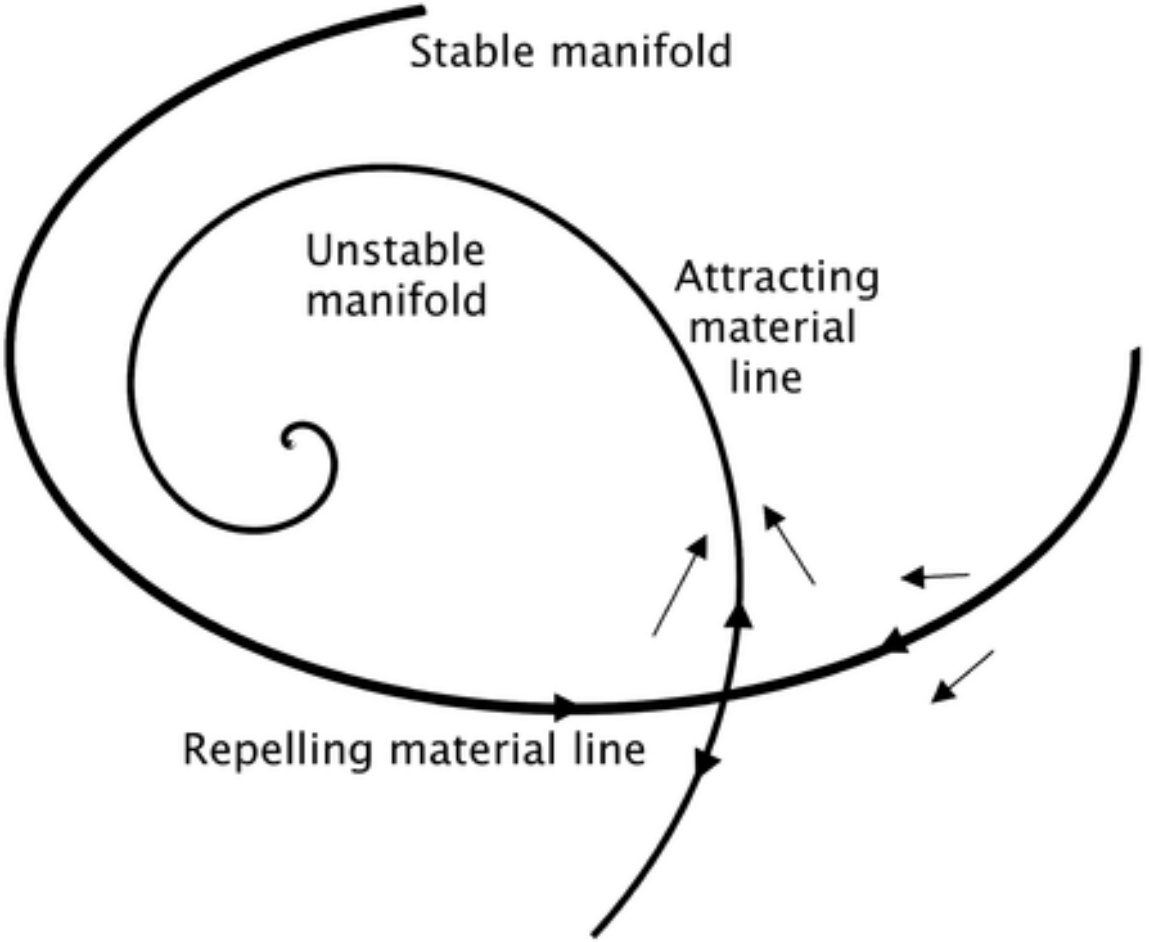

Hyperbolic vortex schematic for an x-y planar flow

Why are steady flow streamlines insufficient?

- The translation speed has spatial variation
- The translation speed has temporal variation
- The flow has time dependence
- The time required to compute the stable manifold may make it irrelevant

Example of steady flow errors

- Trajectories in a time-dependent flow may cross streamlines
- Some particles which are separated from the core by streamlines later enter the storm
- Dots indicate particles entering a 2 degree circle around the pouch center within 2 days

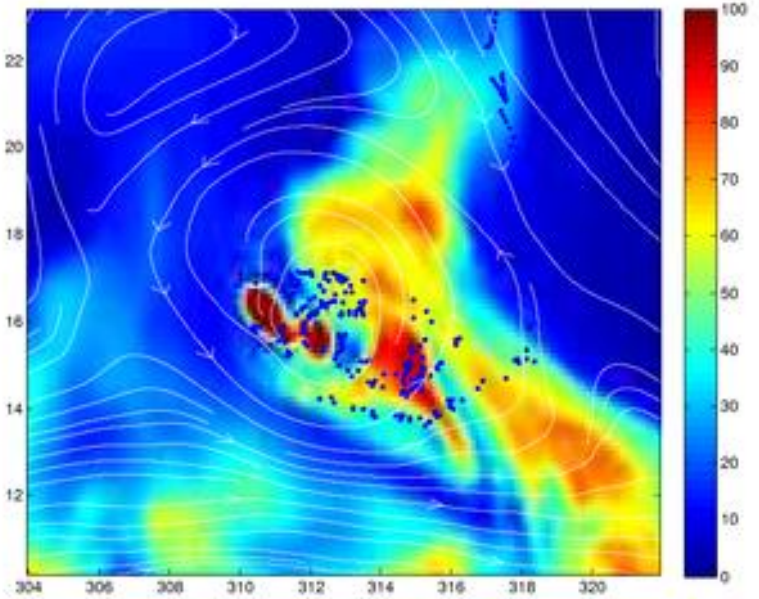

Figure: Streamlines for ex-Gaston in frame of reference at pouch translation speed on Sept. 5 at 0 UTC

Example of sensitivity of streamlines

- Manifolds are sensitive to time and spatial variations in translation speed
- The recirculation is preserved through time-variations in translation speed
- This difference in translation speed can influence the source of air entering the storm

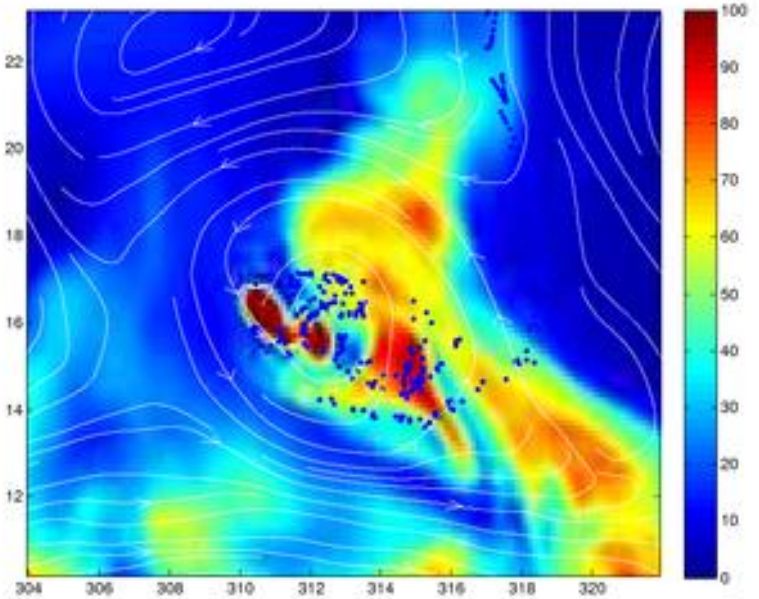

Figure: Streamlines in frame of reference of pouch translation speed at Sept 5 12 UTC

Assumptions made for this simplification

Simplifications of the marsupial paradigm

1. Layerwise two-dimensional flow
2. Steady flow in the translated frame of reference

Simplifications for this study

- The layerwise two-dimensional assumption is still used
- The flow is time-dependent in the translated frame
- Subtracting the translation speed introduces additional sensitivities in stagnation point location and streamline structure
- Lagrangian methods locate boundaries independent of translation speed

Lagrangian methods and trajectory methods for genesis

Trajectory based approaches average the time-variation and locate the structures which do constrain particle movement and form important boundaries.

These methods can be categorized as

- Finite-time scalar field methods
- Trajectory based tracers
- Trajectory statistics

Finite-time Lagrangian techniques

- In a time dependent flow, the most persistent boundaries show linear instability for the longest times
- Finite-time Lagrangian methods efficiently locate boundaries in time-dependent flows
- Direct manifold computation (Haller 2001) utilizes maximal separation of nearby trajectories without relying on stagnation points (Galilean invariance).
- Finite-time Lyapunov exponents (FTLEs) are a commonly used Lagrangian technique.
- Attracting and Repelling Lagrangian coherent structures (LCSs) are detected under backward/forward integration time resp.

FTLE definition

Let $\mathbf{x}$ be an initial point.
Let $\delta\mathbf{x}$ be a perturbation.
$\mathbf{y} = \mathbf{x} + \delta\mathbf{x}$

Growth of perturbation

$$\delta\mathbf{x}(T) = \phi_{t_0}^{t_0+T}(\mathbf{y}) - \phi_{t_0}^{t_0+T}(\mathbf{x}) = \frac{d\phi_{t_0}^{t_0+T}(\mathbf{x})}{d\mathbf{x}}\delta\mathbf{x}(0) + \vartheta(\|\delta\mathbf{x}(0)\|^2).$$

The Euclidean norm of the perturbation is

$$\|\delta\mathbf{x}(t)\| = \sqrt{\left\langle \delta\mathbf{x}(0), \frac{d\phi_{t_0}^{t_0+T}(\mathbf{x})^*}{d\mathbf{x}} \frac{d\phi_{t_0}^{t_0+T}(\mathbf{x})}{d\mathbf{x}}\delta\mathbf{x}(0) \right\rangle}$$

The Cauchy-Green deformation tensor is defined as

$$\Delta = \frac{d\phi_{t_0}^{t_0+T}(\mathbf{x})^*}{d\mathbf{x}} \frac{d\phi_{t_0}^{t_0+T}(\mathbf{x})}{d\mathbf{x}}$$

FTLE definitions (cont.)

Growth is maximal in the maximum eigendirection of Δ

$$\max_{\delta\mathbf{x}(0)} \|\delta\mathbf{x}(T)\| = \sqrt{\lambda_{max}(\Delta)}\, \|\overline{\delta\mathbf{x}}(0)\|$$

$$\max_{\delta\mathbf{x}(0)} \|\delta\mathbf{x}(T)\| = e^{\sigma_{t_0}^{T}(\mathbf{x})|T|}\, \|\overline{\delta\mathbf{x}}(0)\|$$

The FTLE is defined as

$$\sigma_{t_0}^{t_0+T} = \frac{1}{2\,|T|} \log \lambda_{max}(\Delta)$$

The FTLEs are computed as a field for a grid of initial conditions

Example of FTLEs

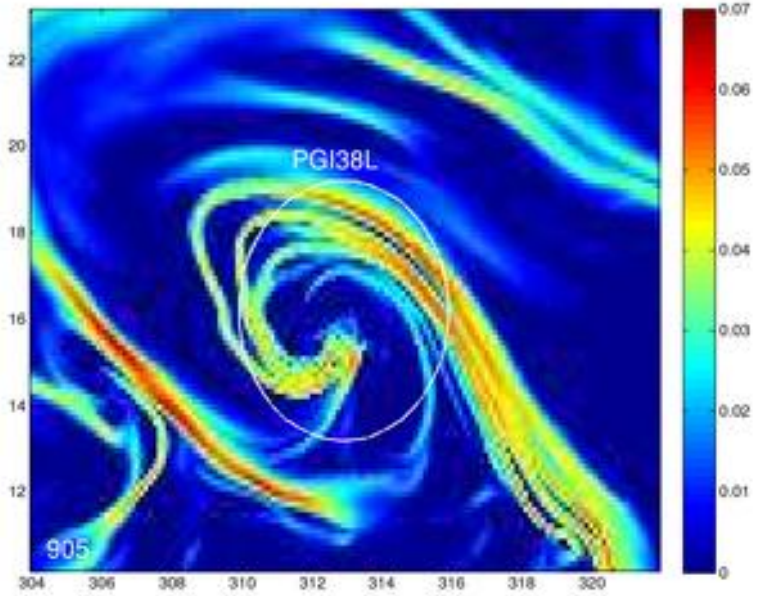

Figure: Backward time FTLE field showing attracting LCSs for ex-Gaston on Sept. 5

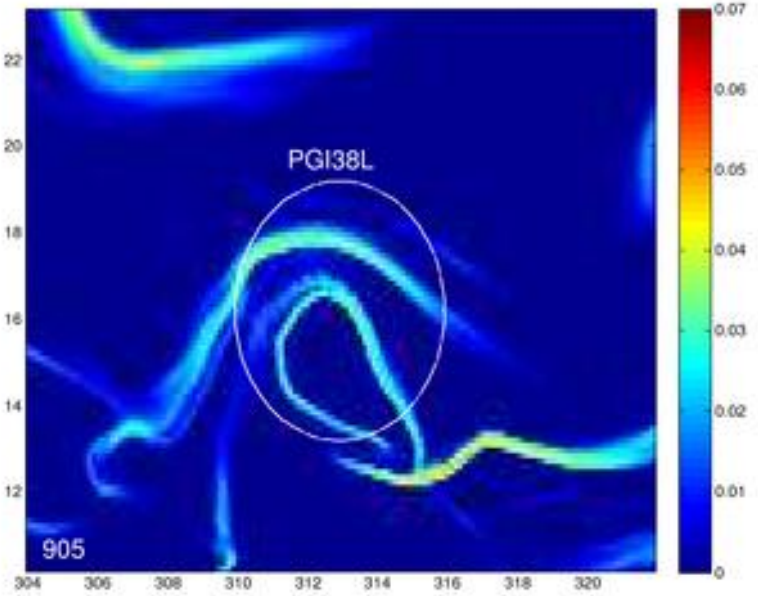

Figure: Forward time FTLE field showing repelling LCSs for ex-Gaston on Sept. 5

Finite-time Lagrangian methods in genesis cases

Model output data

We use ECMWF 25 km resolution analysis data incorporating dropsonde observations

Observations from Lagrangian techniques

- Lagrangian coherent structures persist through time-dependence
- LCSs are well resolved in a 48 hour (backward) integration time
- Attracting LCSs are better resolved than repelling LCSs due to a separation of time scales between the stable and unstable direction
- Repelling LCSs appear to play a critical role when they appear in the inner core

Relation of Lagrangian fields and tracer fields

- Tracer fields show similarity to Lagrangian fields.
- LCSs occur along high tracer gradients, which indicates that maximal linear instability occurs along boundaries of physically different regions.
- Advection is the primary mechanism for the import of air into the pouch under these time intervals. (i.e. minimum diffusion)
- The tracer field can show physical properties of material entering or exiting the pouch.

FTLE and tracer fields

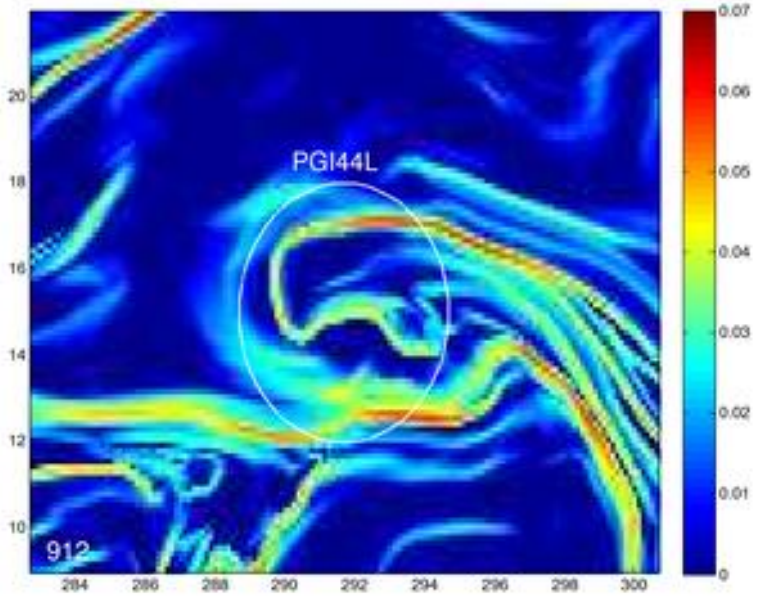

Forward time FTLE field showing repelling LCSs for pre-Karl on Sept 12

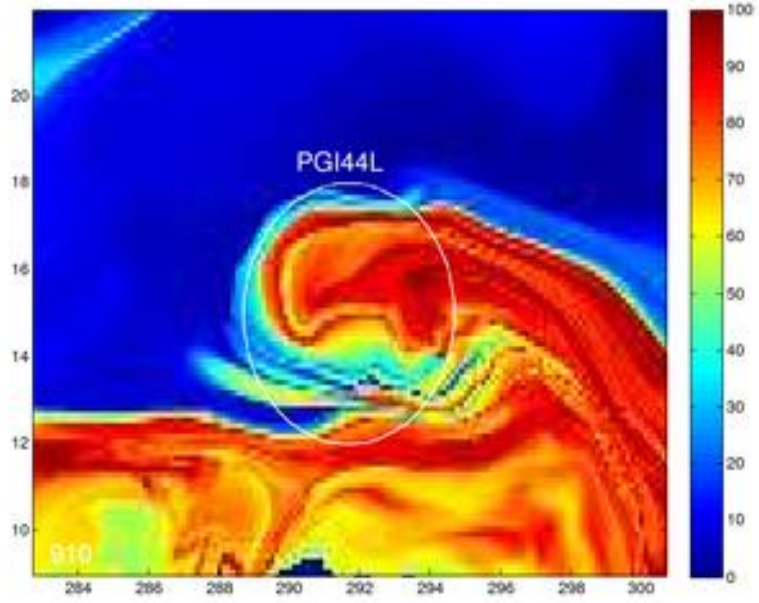

Relative humidity in the Lagrangian frame for pre-Karl on Sept 12

nondevelopment of ex-Gaston

- Gaston was trackable on Aug 28 and declared a TD on Sept 1
- Gaston had increasing moisture at lower levels
- Drying occurred at mid and upper levels beginning Sept 1

Role of LCSs in the non-development of ex-Gaston

- The LCSs explain how Gaston was cut off from the ITCZ moisture source
- The LCSs allow low vorticity dry air to enter the pouch
- A repelling LCS emerges at 700 hPa and above which allows moist air with high vorticity to exit the pouch

Evolution of ex-Gaston

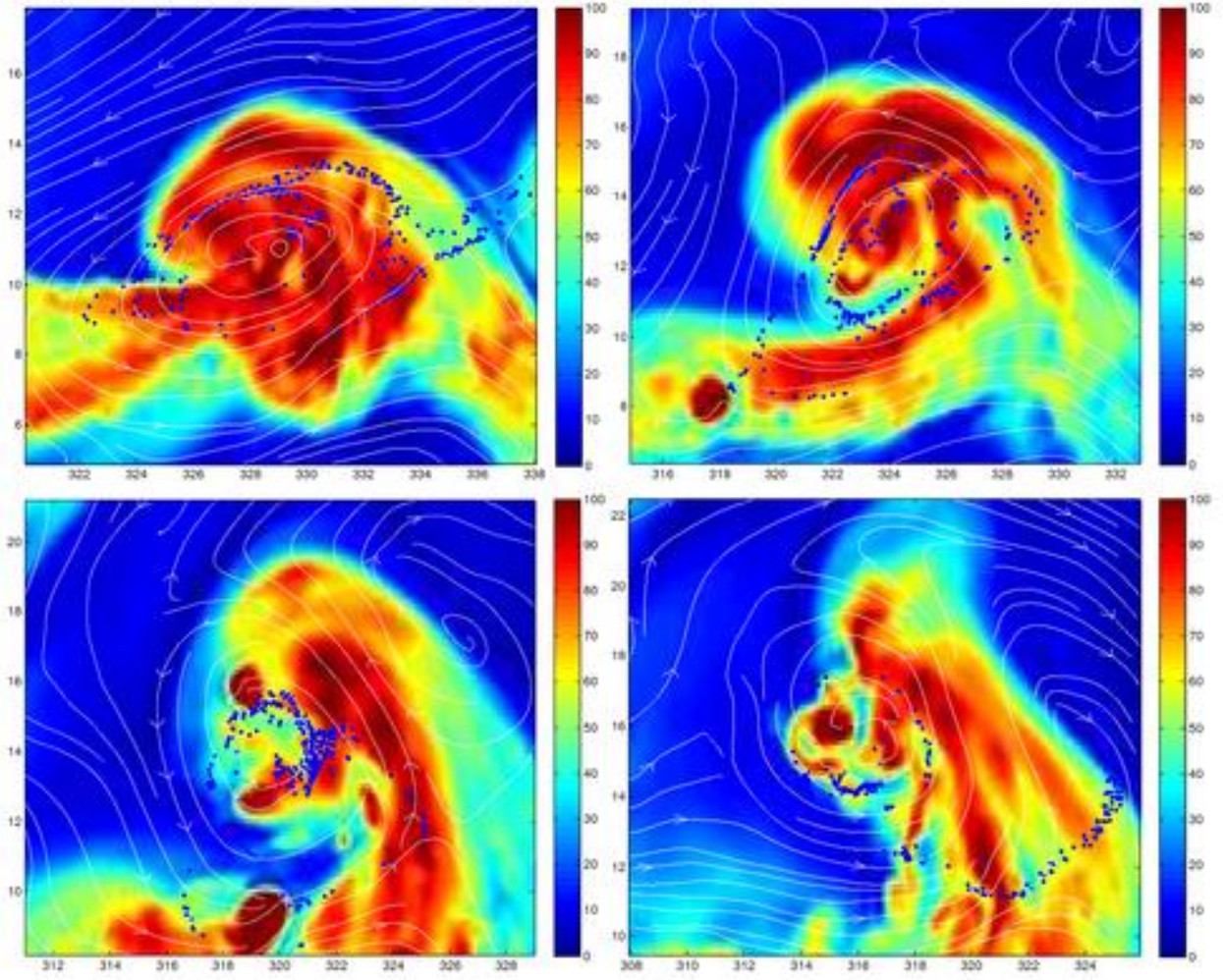

Relative humidity, trajectories and streamlines from 9/01 to 9/04

Evolution of ex-Gaston

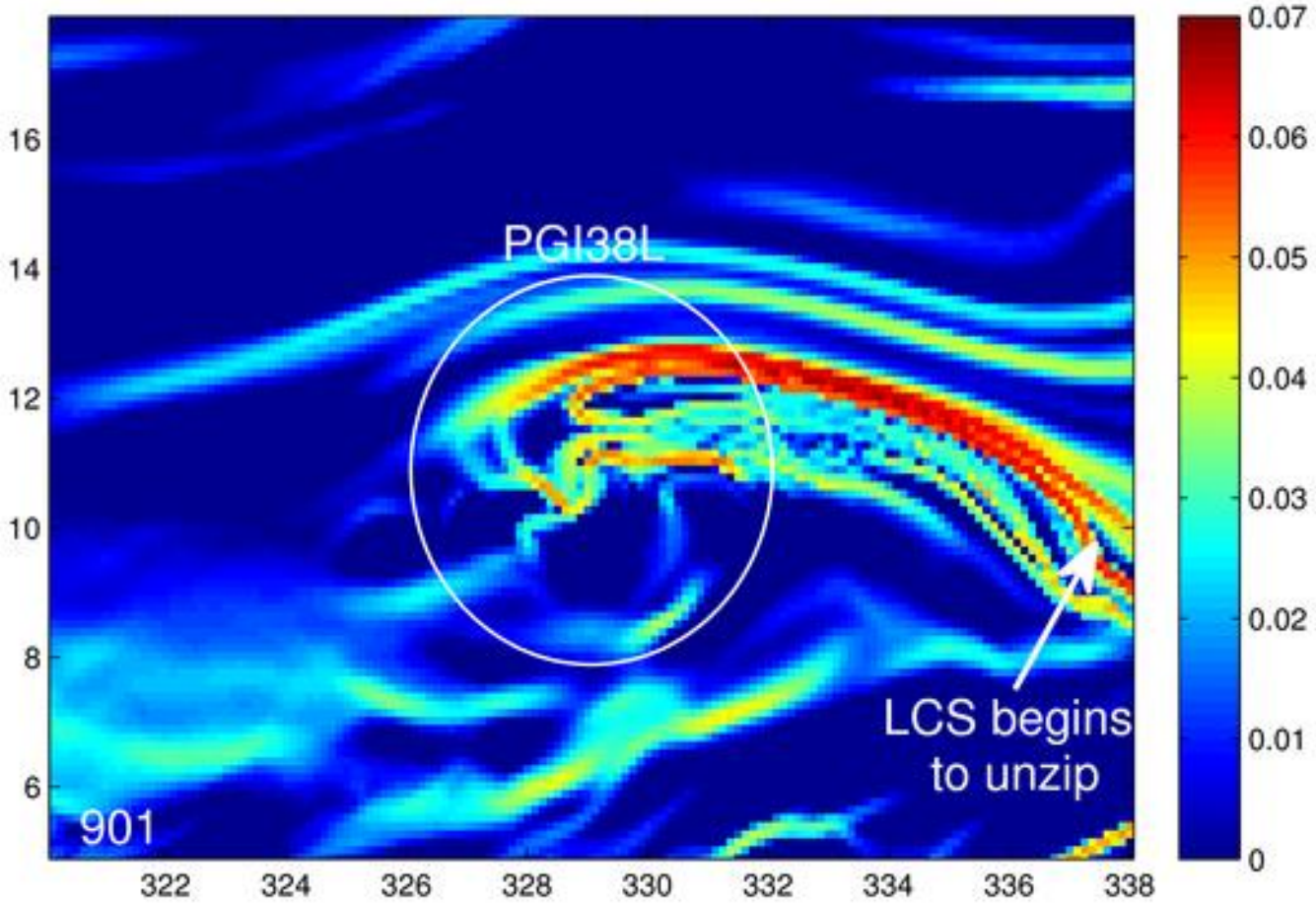

FTLE field showing attracting LCS

Evolution of ex-Gaston

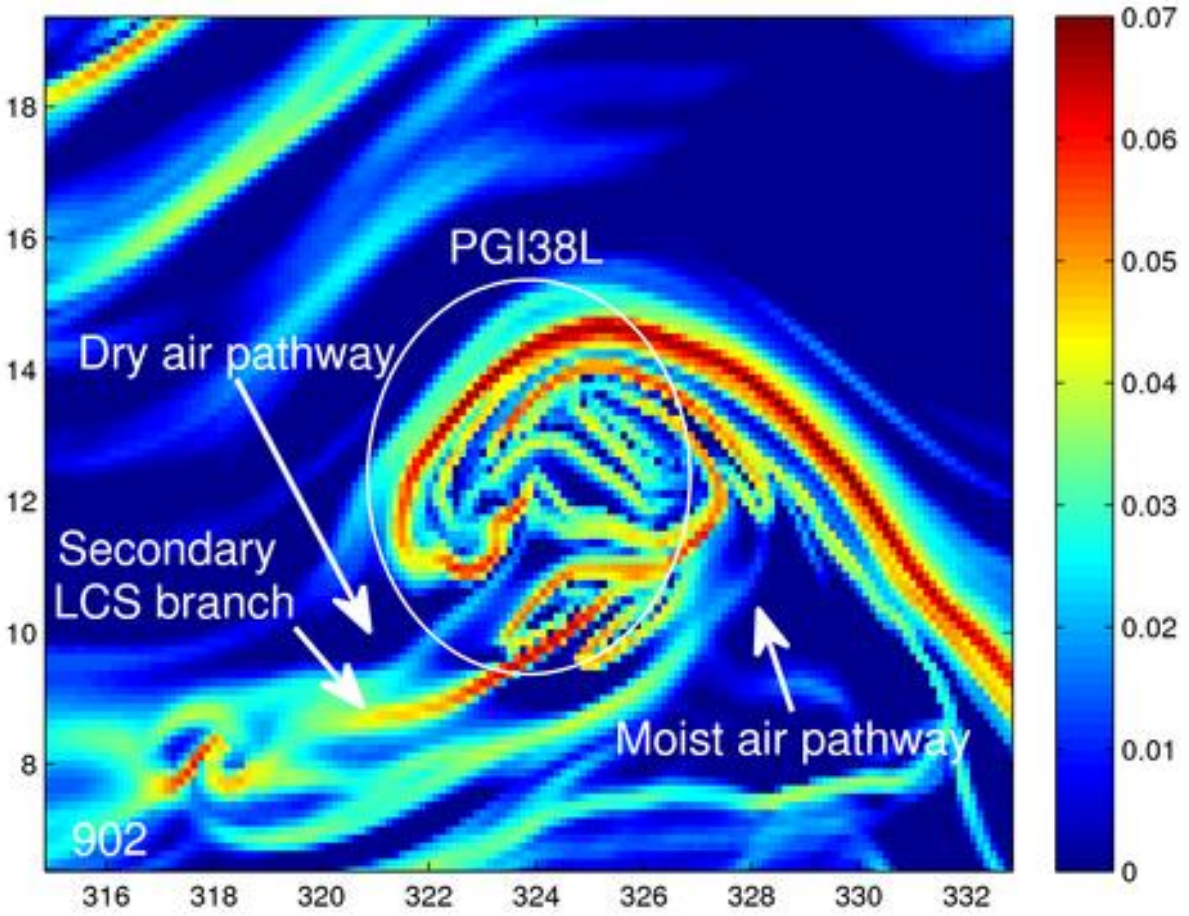

FTLE field showing attracting LCS

Evolution of ex-Gaston

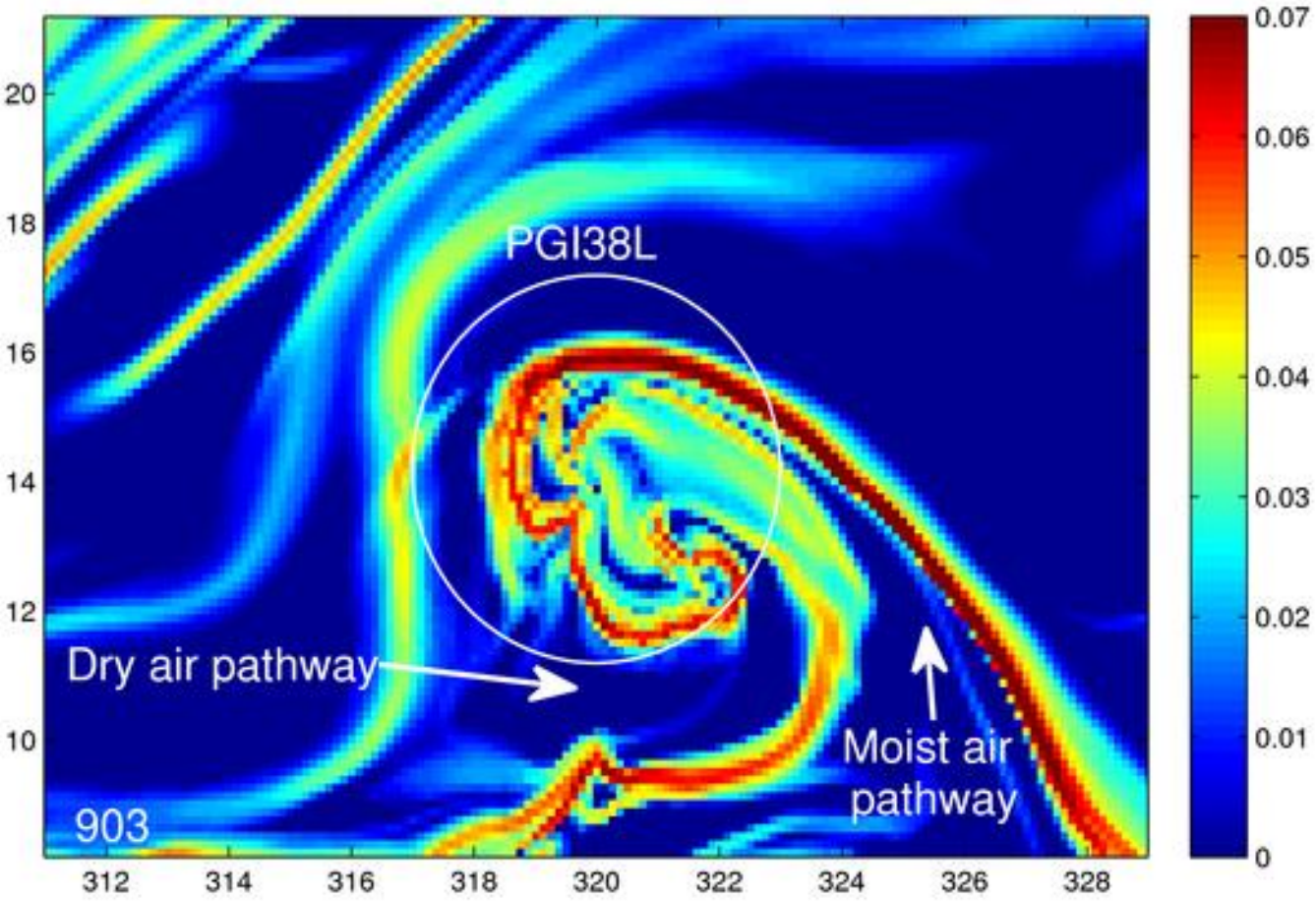

FTLE field showing attracting LCS

Evolution of ex-Gaston

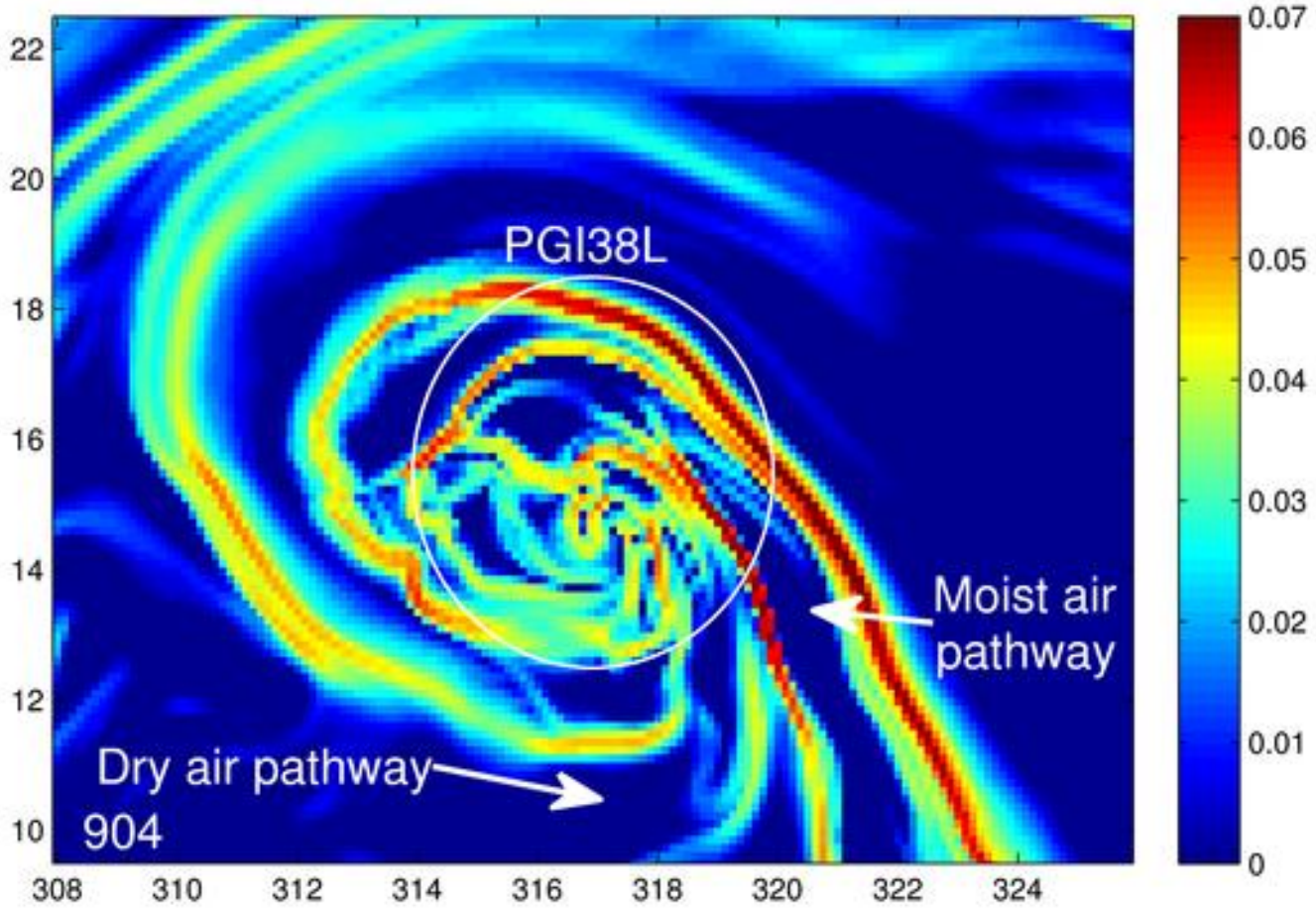

FTLE field showing attracting LCS

Gaston FTLE movie at 700 hPa

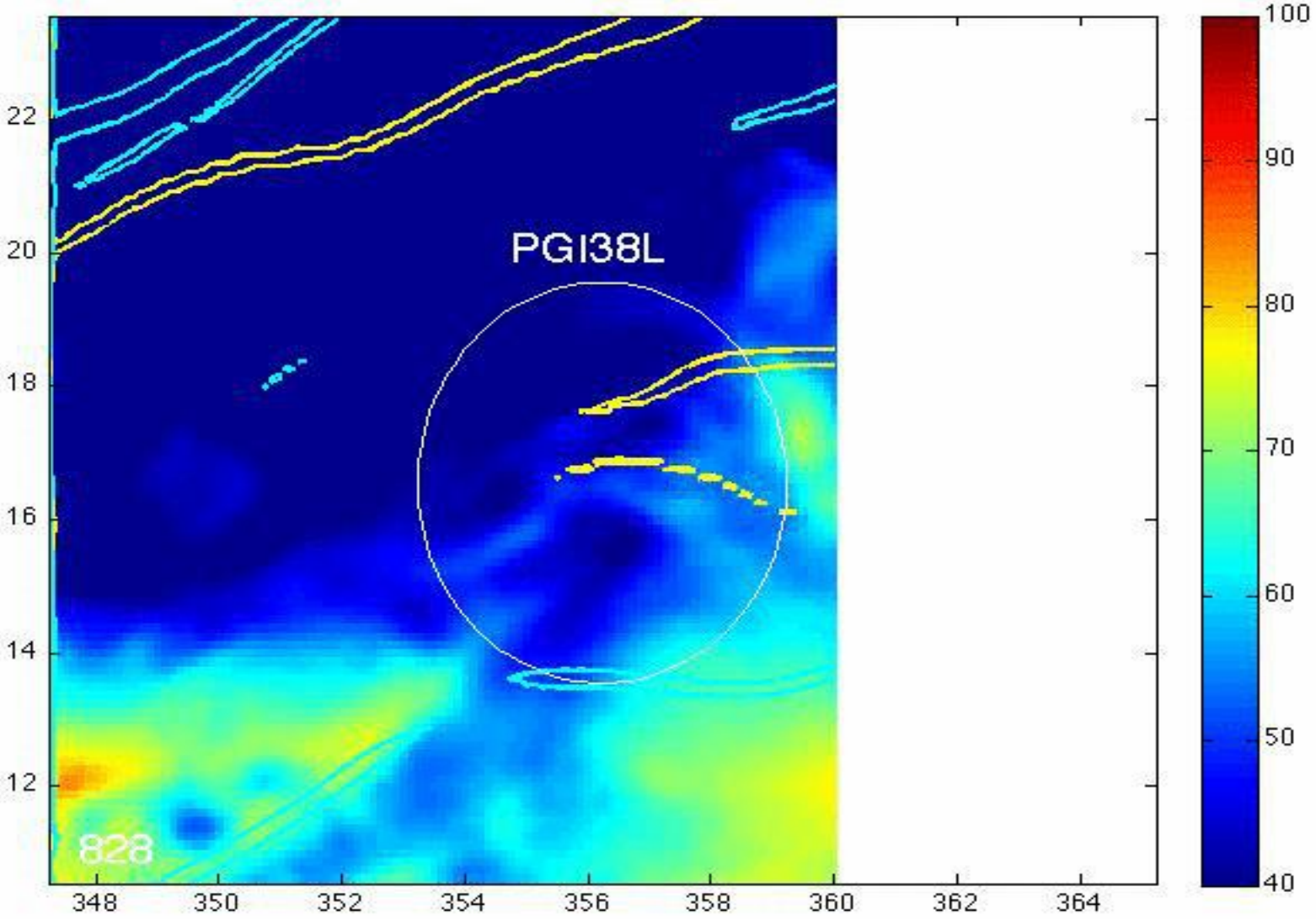

Gaston FTLE movie at 925 hPa

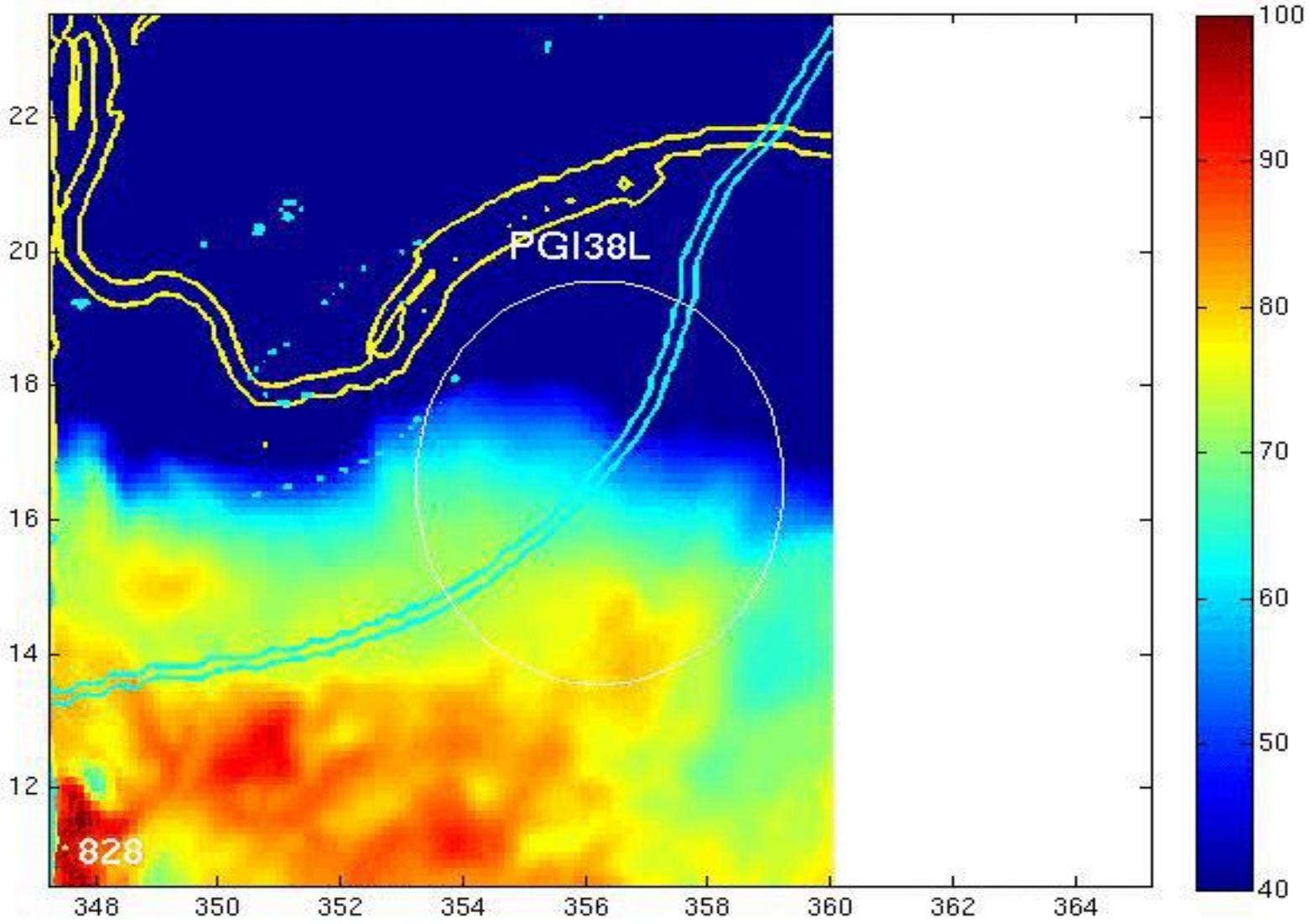

Evolution of ex-Gaston

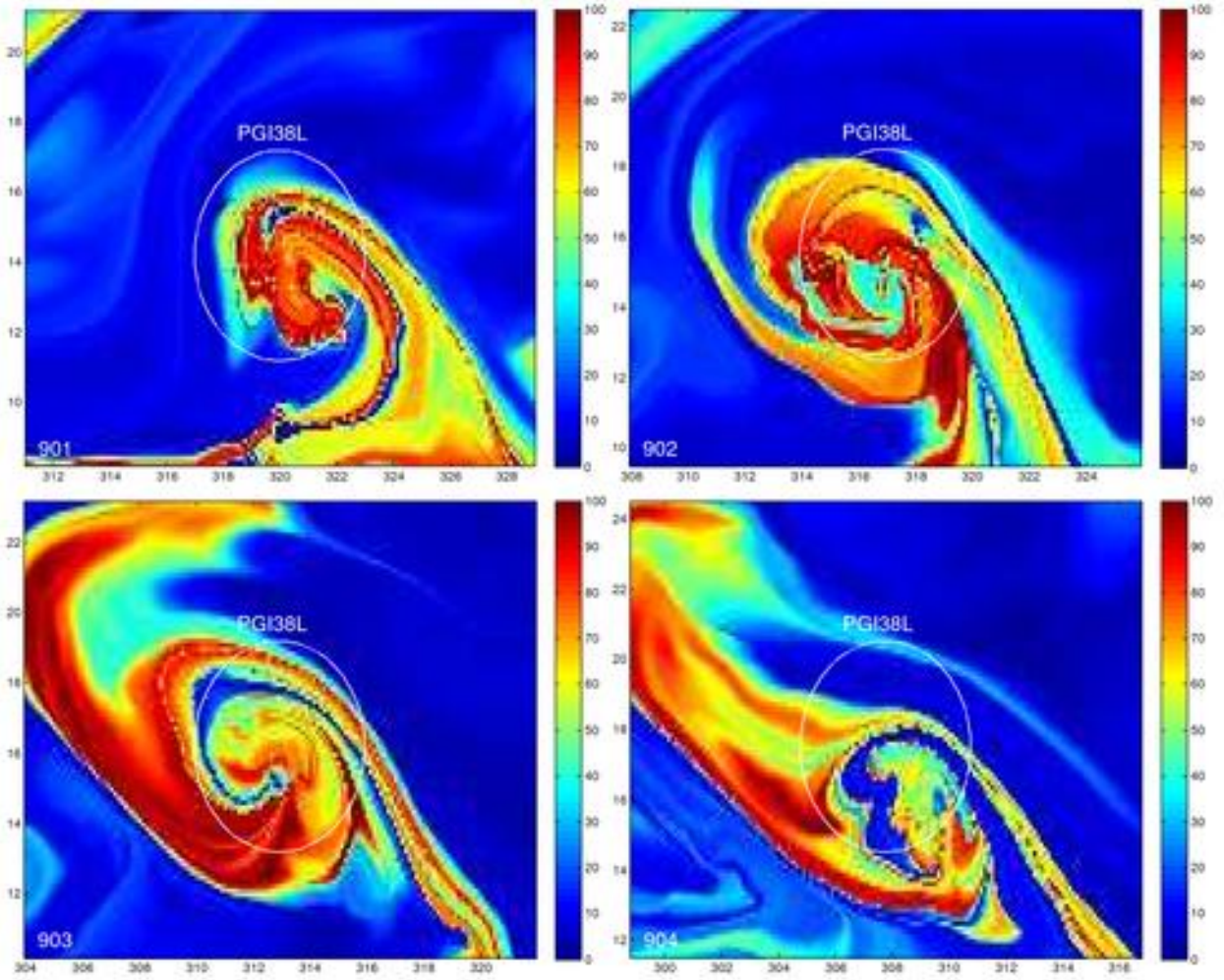

RH values from 9/01 to 9/04 at locations from 9/03 to 9/06

What killed Gaston?

- The pouch is ripped apart beginning Sept. 2
- Net Lagrangian outflow begins at 700 hPa and above

A new Lagrangian criteria for non-development:

A repelling LCS emerges in the pouch center as the pouch is turned inside out

Gaston repelling LCSs at 700 hPa

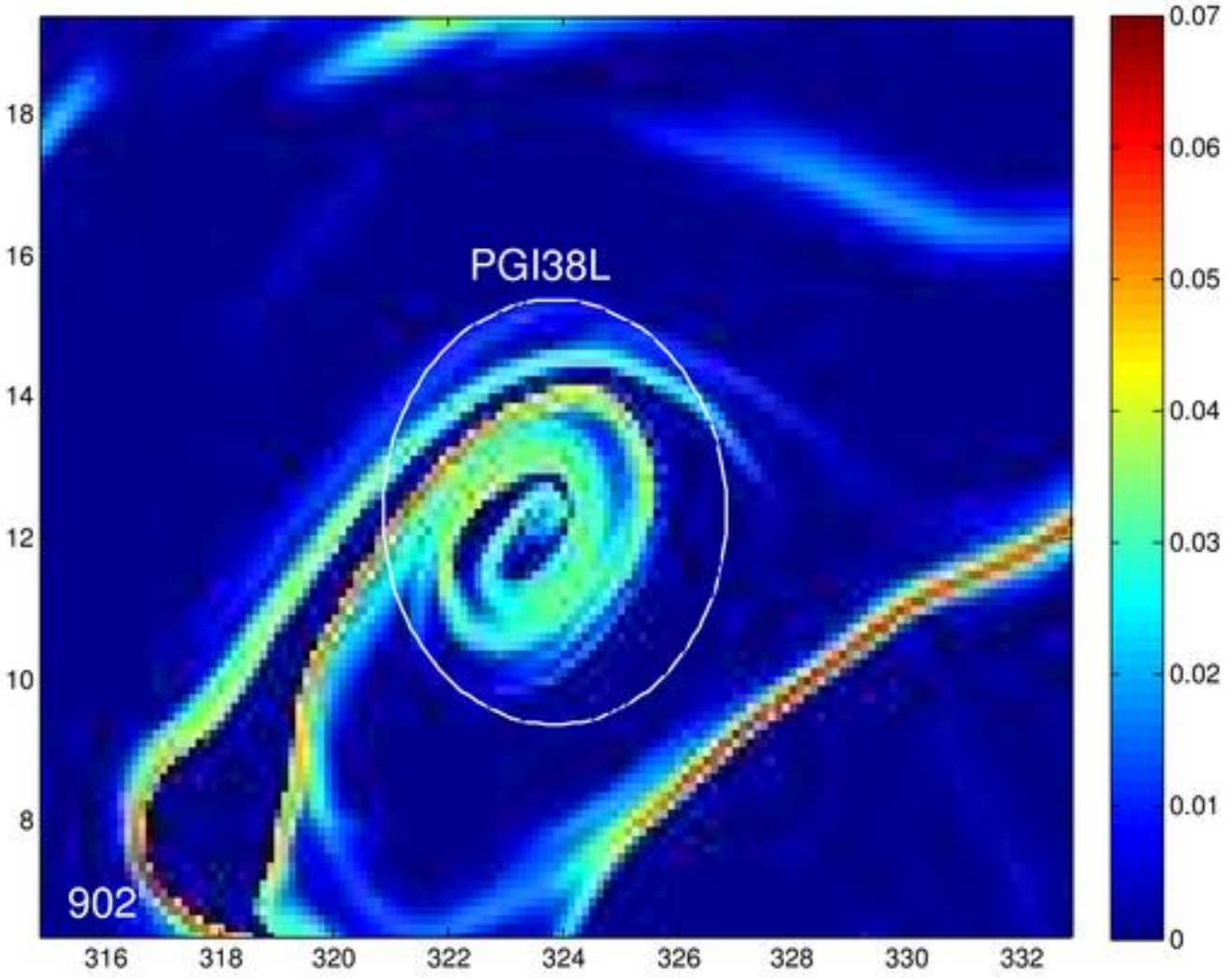

FTLE field showing repelling LCS which emerges at 700 hPa on Sept. 2

Repelling LCS

- Repelling boundaries are strong enough to turn the pouch inside out when their time scale exceeds the time scale along attracting boundaries
- The presence of a repelling boundary precedes the vortex being ripping apart
- A repelling LCS in the core appears for ex-Gaston at 700 hPa (and above)
- The repelling LCS can be seen in the mean FTLE values

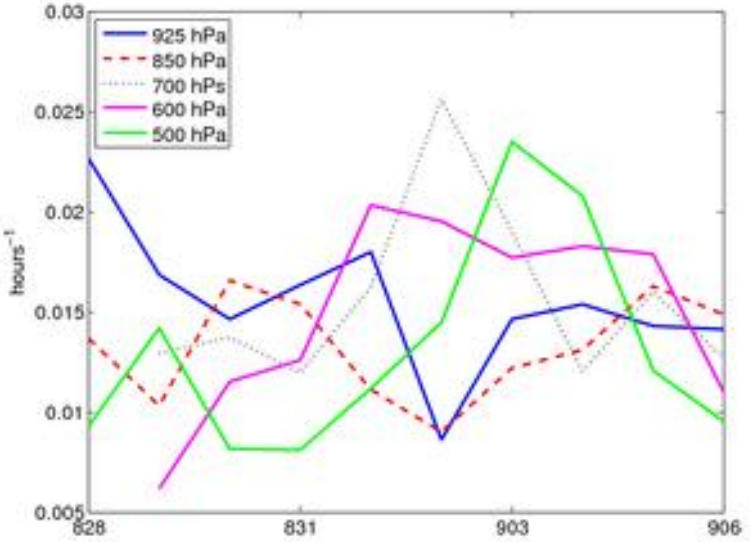

Figure: Average forward time FTLE values for ex-Gaston

Ex-Gaston LCS summary

Reasons for drying at 700 hPa and above

1. Intrusion of dry air from the north
2. Expulsion of moisture to the west
3. Removal of moisture source from ITCZ
4. Presence of a repelling LCS

RH

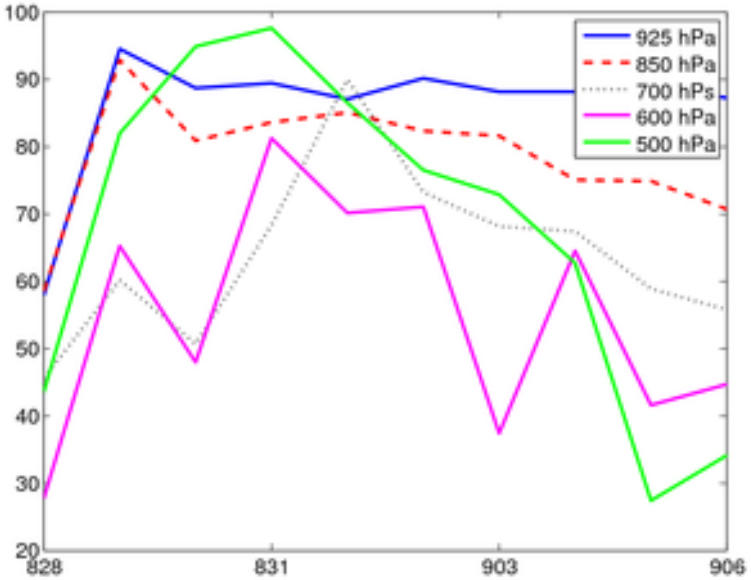

Figure: Pouch average RH at 700 (blue), 850 (red) and 925 hPa (black).

Evolution of vortex strength

Weakening at 700 hPa

- As humidity is removed, OW values decrease at 700 hPa
- The profile remains favourable at lower levels
- Vorticity shows a similar weakening as OW
- Vortex boundaries occur in regions of negative OW
- Cyclonic vorticity is expelled

OW

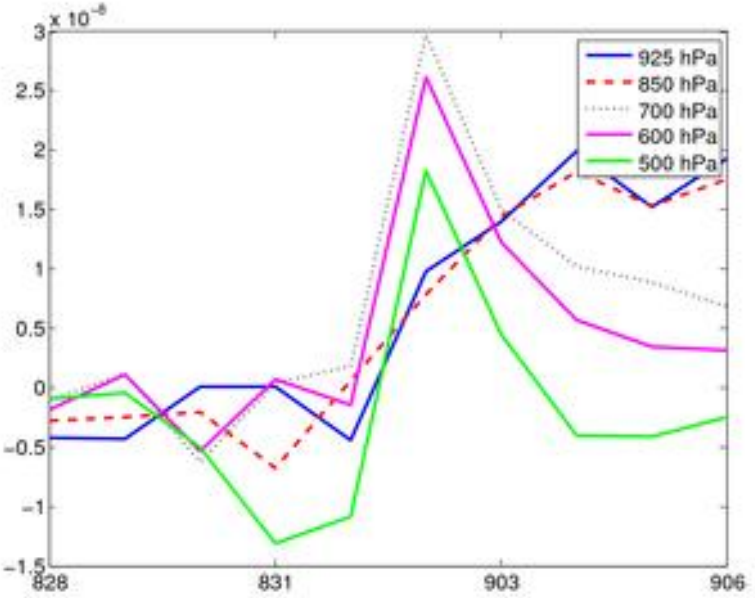

Figure: Pouch average OW at 925 (blue), 850 (red) and 925 hPa (black), 600 (magenta), and 500 (green).

Evolution of pre-Karl

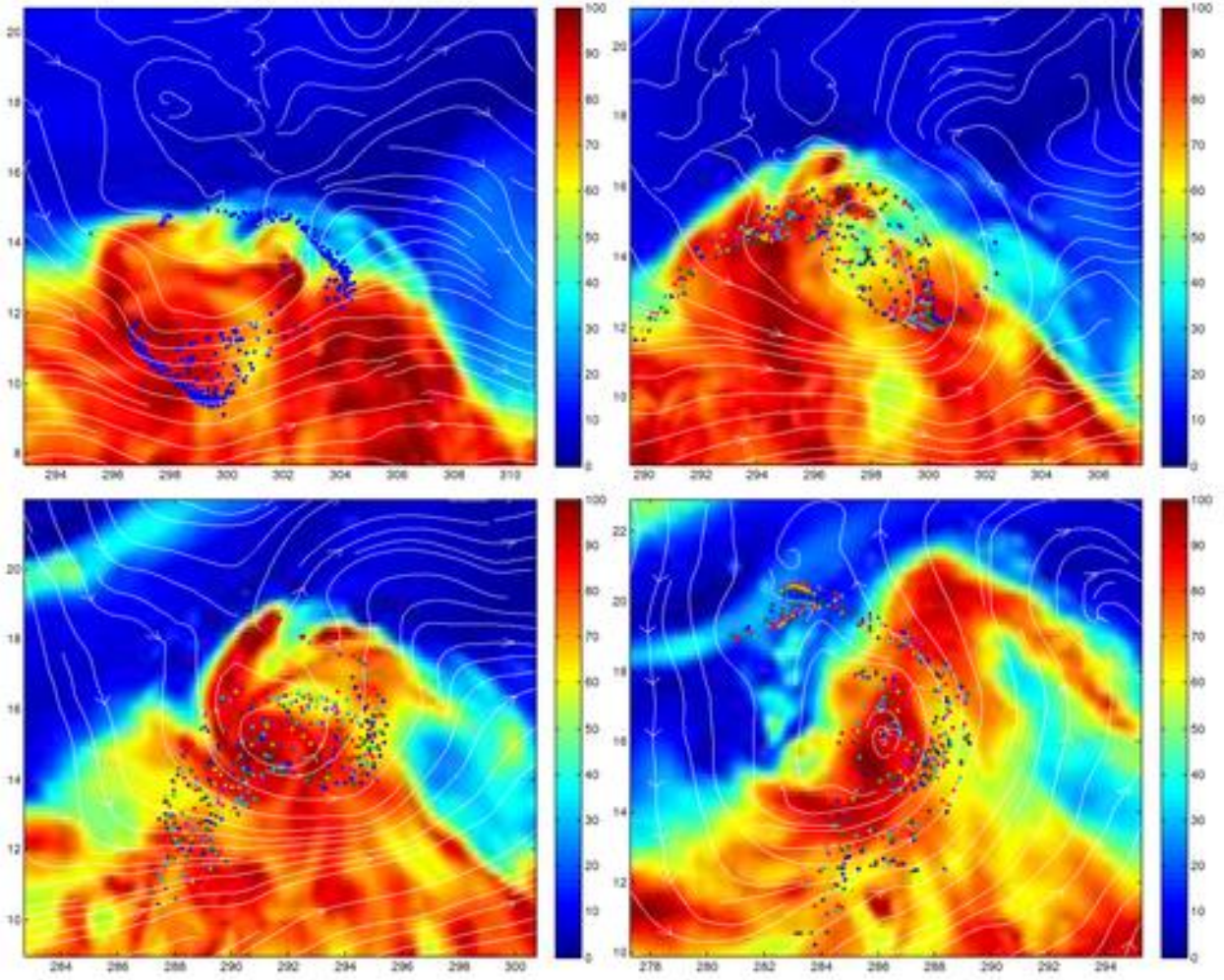

Relative humidity, trajectories, and streamlines from 910 to 913

Evolution of pre-Karl

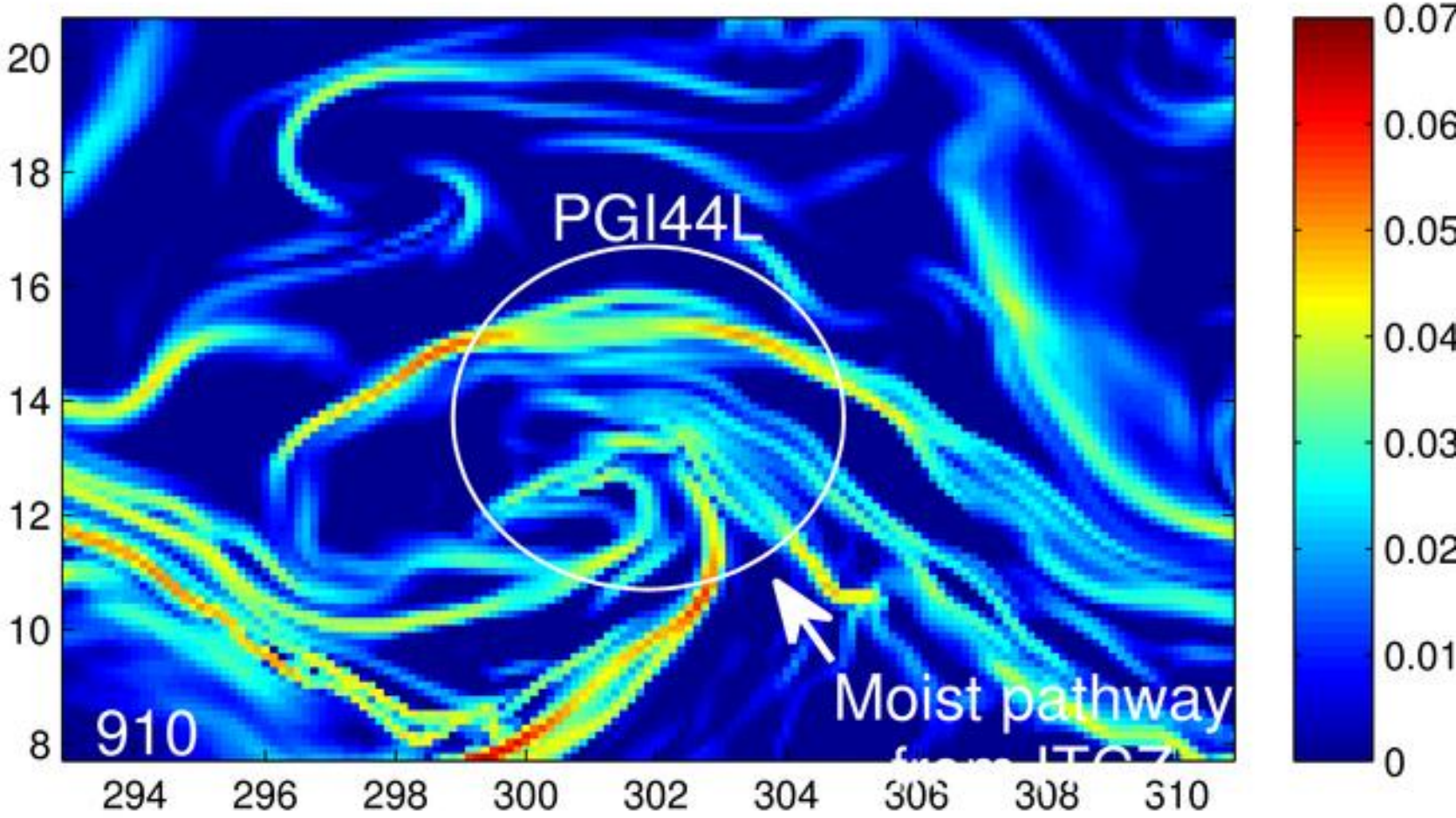

Evolution of pre-Karl

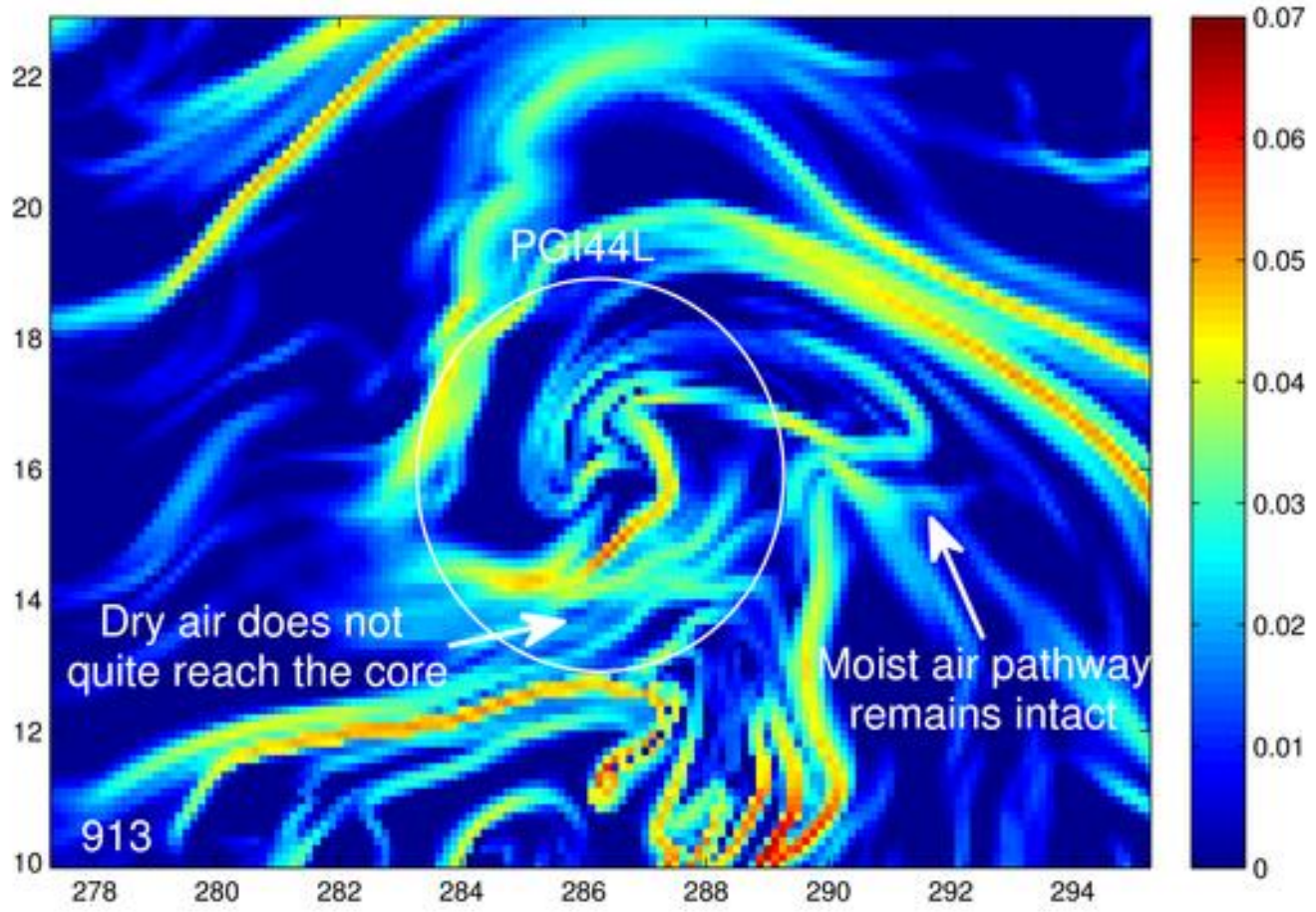

FTLE field showing attracting LCS

pre-Karl LCSs and RH at 700 hPa

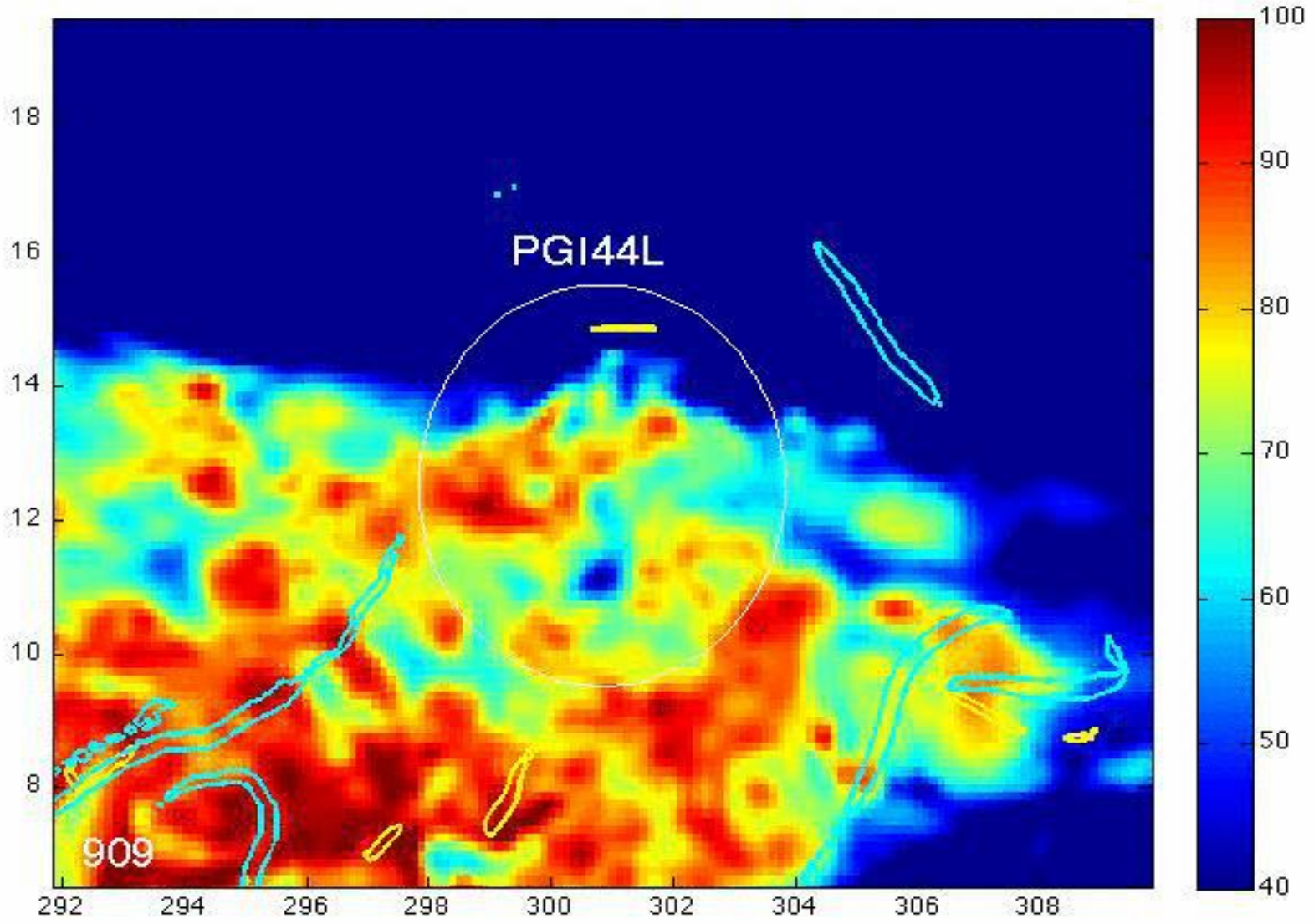

Evolution of pre-Karl

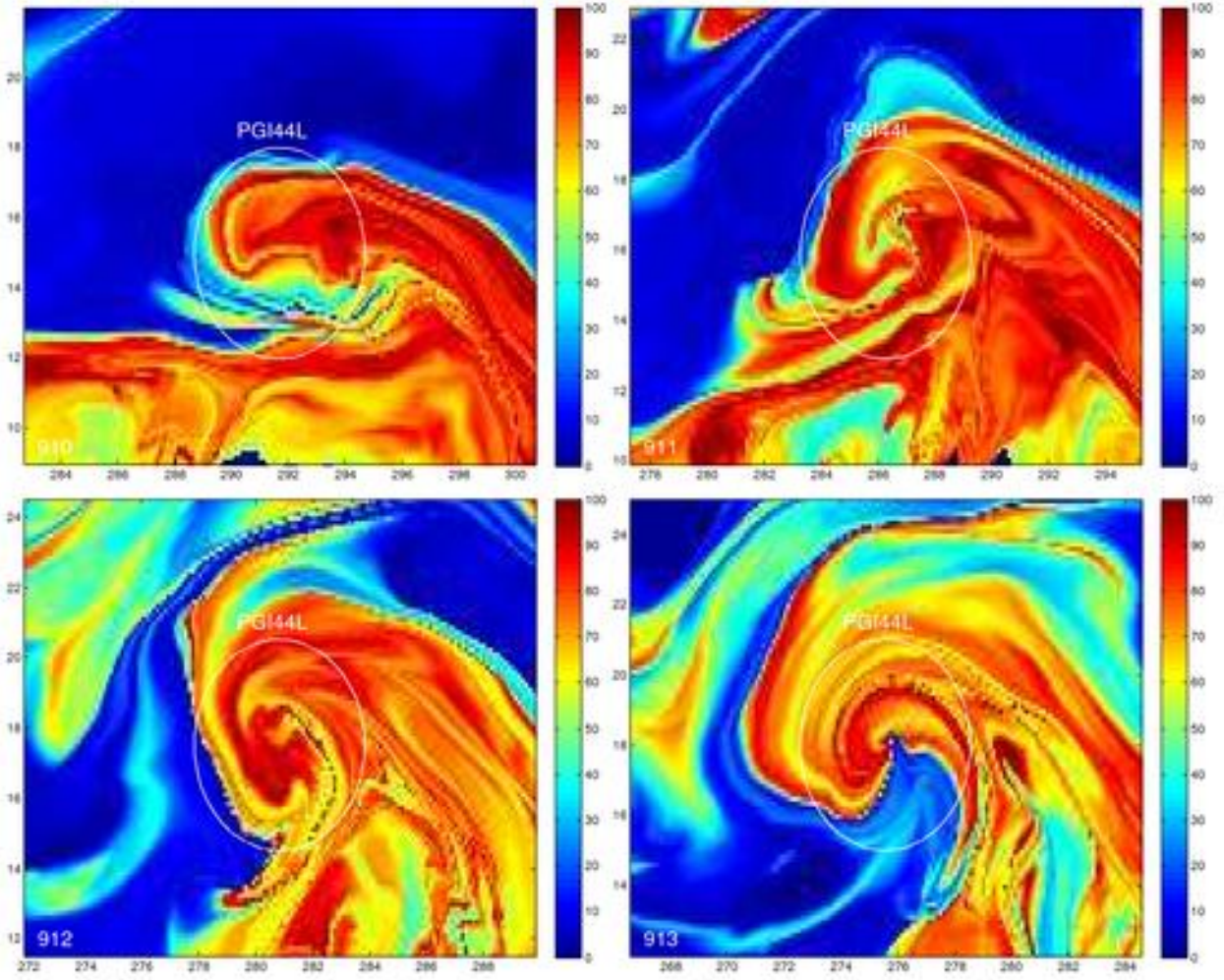

Relative humidity field in the Lagrangian frame from 9/10 to 9/13

Karl's continued pathway to the ITCZ

Moistening at 700 hPa

1. Exclusion of dry air from the north
2. Little ventilation of moisture to the west
3. Maintenance of moisture source from ITCZ

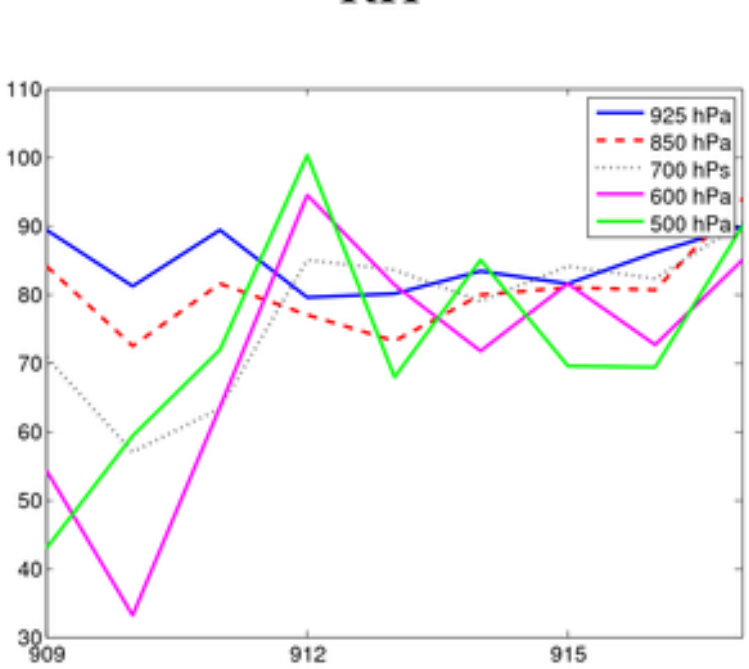

Figure: Pouch average RH at 700 (blue), 850 (red) and 925 hPa (black).

Vortex strength of pre-Karl

OW profile

1. Increase in vortex strength occurs as humidity increases
2. The vortex overcomes the influence of dry air that reaches the edge of the pouch

OW

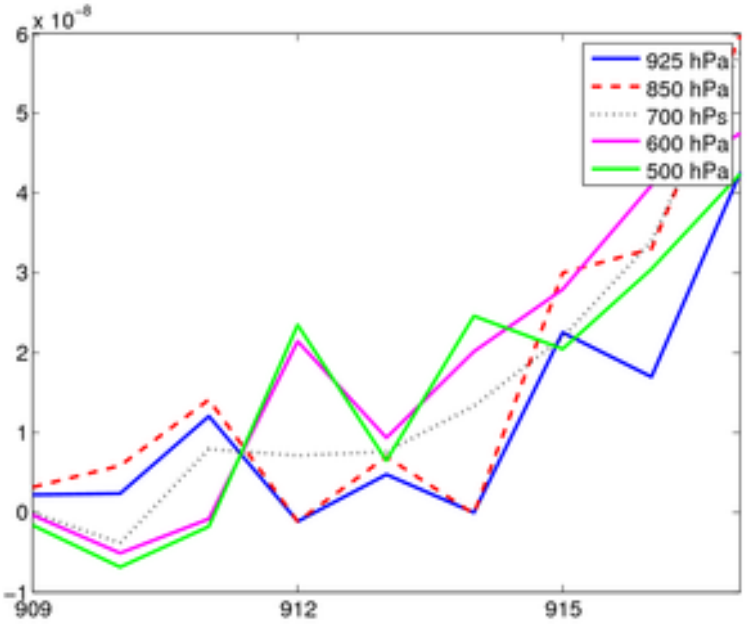

Figure: Pouch average OW at 925 (blue), 850 (red), 700 hPa (black), 600 (magenta), and 500 (green).

pre-Karl lessons learned

- There is no repelling LCS in the pouch
- The attracting LCS remains intact
- Dry air does not penetrate the core as quickly
- The moisture path from the ITCZ remains intact
- The LCSs form a persistent boundary for dry air to the north
- The dynamical resilience of the vortex overcomes adverse conditions outside of the pouch

Conclusions

- Lagrangian boundaries persist through the time-dependent flow
- The LCSs are invisible in Eulerian fields
- Moisture is constrained by the Lagrangian boundaries

Why Gaston did not form

A boundary that unzips cuts off the flow of moisture from the ITCZ

This LCS begins to deform 2 days before the moisture source is removed

Dry air intrudes at mid levels

Karl was able to resist the adverse conditions at mid-levels and was able to keep out dry air

Future outlook

- Further studies from 2010 storms Matthew, Nicole, Fiona, and Alex
- Relationship between LCSs and thermodynamics
- Development of LCS products as a diagnostic and forecasting tool
- Use of Lagrangian methods on 3D data